Hindawi
Advances in Materials Science and Engineering
Volume 2019, Article ID 4853102, 7 pages
https://doi.org/10.1155/2019/4853102

Research Article

Dynamic Response Law of Loess Slope with Different Shapes

Zhixin Yan,[1,2] **Sen Zhang**,[1,3] **Xuedong Zhang**,[1,4] **and Ping Jiang**[1]

[1]*School of Civil Engineering and Mechanics, Lanzhou University, Lanzhou 730000, China*
[2]*School of Civil and Transportation Engineering, Henan University of Urban Construction, Pingdingshan 467036, China*
[3]*Yunnan Research Institute of Highway Science and Technology, Kunming 650051, China*
[4]*China Water Resources Beifang Investigation, Design and Research Company Limited, Tianjin 300222, China*

Correspondence should be addressed to Sen Zhang; 97672627@qq.com

Received 16 November 2018; Accepted 17 February 2019; Published 25 March 2019

Academic Editor: Paweł Kłosowski

Loess slope broadly distributes in Northwest China, making the slope of the area developed. And with the development number of construction projects still on the rise, this area is a high-intensity region with multiple earthquakes, resulting in landslide under earthquakes which is a very serious problem. However, the study on the loess slope dynamic response yet rarely involved the exploration of the influence of slope shapes, which leaves a hidden danger to the safety of local engineering. In this paper, a typical ladder-type loess slope in engineering is selected as a research object, and a numerical simulation model is established with FLAC3D program. The dynamic response of the loess slope with different shapes is studied deeply and systematically. Found a series phenomenon of earthquake response of loess slope with stepped slope series, the width of the platform and the slope ratio change under earthquakes. Meanwhile, the law of slope parameters such as slope series, platform width, and slope ratio on dynamic response of loess slope is revealed. The results provide theoretical support and scientific basis for the construction of the relevant projects in the area, which has important reference value to the safety of the engineering and the development of economic society.

1. Introduction

Loess is a kind of porous and weakly cemented quaternary sediment widely distributed in the Northwest China. It has a large thickness, complete loess strata, many geomorphologic types, and complex landforms, which make the slope of this area develop in large quantities. As the number of loess slopes is growing rapidly with the development of engineering construction and high-intensity earthquakes are common in the Northwest China, serious earthquake-induced landslides have been caused there. However, the study of dynamic response of the loess slope is still in the exploratory stage. Therefore, research on the seismic dynamic response of loess slopes with different shapes according to the needs of engineering construction in a loess region is of great significance for engineering safety and economic and social development of the region.

Studying the seismic dynamic response of loess slopes with different shapes may reveal the influence of slope shape on dynamic stability and dynamic failure mechanism of loess slope and provide scientific basis for engineering construction. The factors affecting the dynamic response, stability, and failure mechanism of the slope include slope's characteristics and ground motion parameters [1]. Scholars have made some research on the stability of loess slope, landslide type, landslide mechanism and motion law of landslide mass under earthquake, and the influence of ground motion parameters on slope stability and landslide damage. Chen et al. [2] obtained the displacement and stress fields and the dynamic stability and safety factors of loess slope by using the quasi-static strength reduction method; Gong et al. [3] tested and analyzed the dynamic response of the loess cutting slope under column hammer vibration; Sun et al. [4] have studied on the occurrence mechanism of typical long-distance loess landslide triggered by Haiyuan earthquake in 1920. Sassa [5] proposed a landslide motion model considering the influence of pore pressure; Wang and Zhang [6] proposed the mechanism of earthquake-induced high-speed loess landslide-loess disintegration, oblique projectile motion, and dust-forming effect of loess mass; Keefer [7] classified seismic landslides into three categories according to motion characteristics and destructive effect

thereof; Prestininzi and Romeo [8] presented the relation between seismic intensity and earthquake-induced landslide; Scheidegger [9] proposed the slide friction model of landslide mass; Jibson and Keefer [10] and Romeo [11] discussed how to determine the acceleration-time history of ground motion using Newmark analysis method; and other scholars studied on the influence of ground motion parameters upon dynamic response of a slope [12–18]. Nevertheless, research on seismic dynamic response of loess slope has up to now seldom focused on the factors related to the slope shape such as slope type and slope ratio, undoubtedly leaving hidden troubles for the safety of engineering construction in the loess regions prone to high-intensity earthquake [19–22]. In this paper, the typical stepped loess slope in engineering construction is taken into consideration as the research object, and the numerical analysis model is established by using FLAC3D software to study the dynamic response of loess slopes with different shapes.

2. Establishment and Loading Scheme of Dynamic Analysis Model for Loess Slope

2.1. Establishment of Analytical Model. To study the general law of seismic dynamic response of loess slope, the slope model in numerical simulation is set as an isotropic homogeneous slope. The parameters of the loess slope include density 1,610 kg/m^3, elasticity modulus 102 MPa, Poisson's ratio 0.3, damping ration 0.15, cohesion 28 kPa, and internal friction angle 30°. An ideal elastoplastic model and Mohr–Coulomb yield criterion are used in the constitutive model and yield criterion of loess, respectively. For the practical value of the research, the parameters of the loess slope are quoted from the engineering examples and the strain in the calculated results is obtained by modeling and calculation.

To establishing the dynamic analysis model, Fast Lagrangian Analysis of Continua (FLAC) is used as the simulation software. In this paper, we use the 3D version to simulate all process. As the loess slope is a semiinfinite body, considering the seismic wave and energy diffusion in dynamic analysis, the periphery of the model is set as a free-field boundary which may absorb some waves propagating outward so that the physical phenomenon at the boundary will conform to reality and no reflection of sound waves will occur. The infinite depth of the lower area of the loess slope is treated by setting the viscous boundary. The scale of the slope model is selected according to standard [23], and the mesh size, which should be less than 1/8 to 1/10 the wavelength corresponding to the highest frequency of input seismic wave, i.e., controlled within 5 m, is set as 2 m in this paper to eliminate the possible influence of the frequency of seismic waves and the wave velocity of loess mass upon the precision of numerical simulation. The established numerical simulation analysis model is shown in Figure 1.

When using the viscous boundary, seismic waves have to be converted into stress-time history input. For this reason, acceleration-time history can be obtained by integrating acceleration-time history, and then the velocity-time history

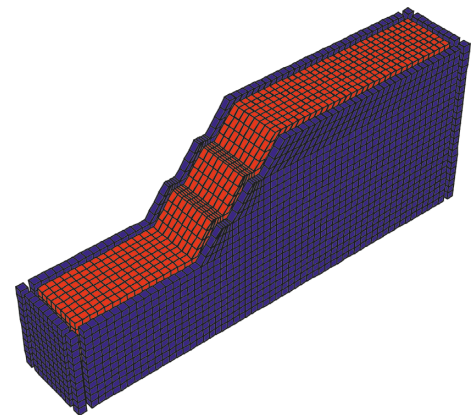

Figure 1: Slope model.

can be transformed into the stress-time history by the following equations:

$$\sigma_n = -2\left(\rho C_p\right)v_n,$$
$$\sigma_s = -2\left(\rho C_s\right)v_s, \quad (1)$$

where σ_n and σ_s denote the normal stress and the shear stress applied on the viscous boundary, respectively; ρ denote the density of the material medium; and C_p and C_s denote the pressure wave velocity and the shear wave velocity, respectively.

2.2. Seismic Wave Processing. The east-west wave of Kobe earthquake with a duration of 41 s and peak acceleration of 2.247 g recorded at the Kakogawa Station of Japan in 1995 is used as the input seismic wave in the numerical simulation. As the energy of the seismic wave is mainly concentrated in the first 20 s, the acceleration records of the first 20 s are intercepted in the the numerical simulation. Then, the time history curve of the captured acceleration is subjected to baseline correction and filtering (to filter high-frequency component above 10 Hz). In addition, the peak value of acceleration is adjusted to 0.15 g according to the fortification intensity of the general building. The velocity-time history curve is obtained by integration as shown in Figure 2.

The effect of dynamic boundary conditions and the correctness of the seismic wave input can be determined by tracking the acceleration-time history near the bottom of the numerical simulation analysis model. In this paper, the Kobe wave is used as the input seismic wave. It can be seen from Figure 3 that the acceleration response-time history curve of the monitoring point at the bottom of the model fits perfectly with the input seismic wave acceleration-time history curve, implying effective simulation of dynamic boundary conditions and correct seismic wave input.

2.3. Numerical Simulation Conditions. To explore the influence of the shape of the loess slope upon the dynamic response, the dynamic response analysis of different width, different slope ratios, and different step numbers were analyzed, as shown in Table 1. At each condition, a series of

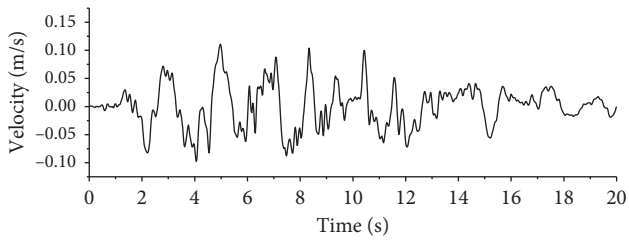

Figure 2: Velocity-time history curve of the Kobe wave.

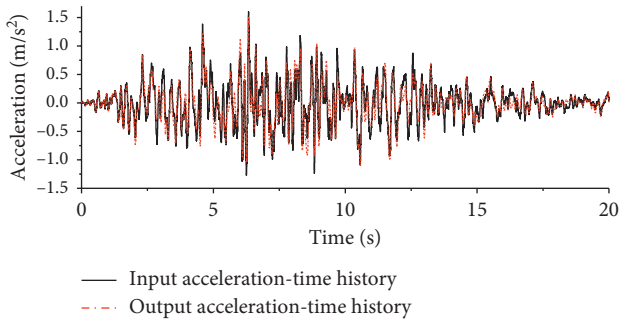

Figure 3: Input and output acceleration-time history curves.

monitoring points are set up on the slope surface at an interval of 2 m from the slope toe to slope top, monitoring points are set up for the multistep slope from the slope toe to slope shoulder of each step. The layout of the monitoring point is shown in Figure 4.

To describe the acceleration response of the slope under earthquake, the ratio of the peak value of dynamic response acceleration at any point within the slope (PGA) to that at slope point O in Figure 4 is defined as the amplification factor of PGA and the ratio of the peak value of dynamic response velocity at any point within the slope (PGV) to that at slope point O in Figure 4, as the amplification factor of PGV. The PGA and PGV are convenient to show the response of any point in the slop to ground motion, and it is easy to quantify the number of magnified points under the same reference point and to see the site which is more easily destroyed.

3. Dynamic Response Analysis of Loess Slopes with Different Steps

To investigate the influence of the loess slope grade on its dynamic response, three conditions, in which the step number to be one (J-1), two (J-2), and three (J-3), are set, respectively, for a 30-meter-high loess slope. The distribution laws of dynamic response acceleration, velocity, and displacement of loess slopes with different steps are obtained through numerical calculation, as shown in Figures 5–7.

It can be seen from Figure 5 that, under Condition J-1, the PGA amplification factor of the J-2 grade loess slope increases with the slope height in general, and the oscillation of the PGA magnification factor is obvious in the range from the slope foot to 2/3 slope height; in the case of J-2 grade slope, the PGA amplification factor of the bench of the first

Table 1: Numerical simulation arrangement about working condition.

Simulation conditions	Slope height (m)	Bench width (m)	Step number	Slope ratio
P-1	30	2	3	1 : 0.75
P-2	30	3	3	1 : 0.75
P-3	30	4	3	1 : 0.75
P-4	30	5	3	1 : 0.75
J-1	30	2	1	1 : 0.75
J-2	30	2	2	1 : 0.75
J-3	30	2	3	1 : 0.75
B-1	30	2	3	1 : 0.5
B-2	30	2	3	1 : 0.75
B-3	30	2	3	1 : 1
B-4	30	2	3	1 : 1.25

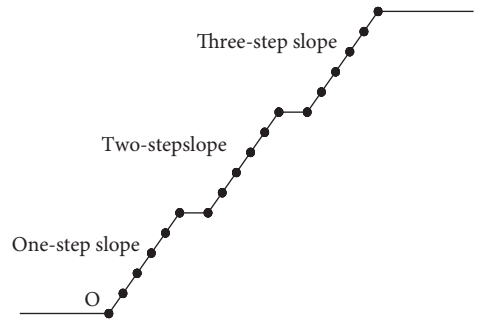

Figure 4: Layout of monitoring points.

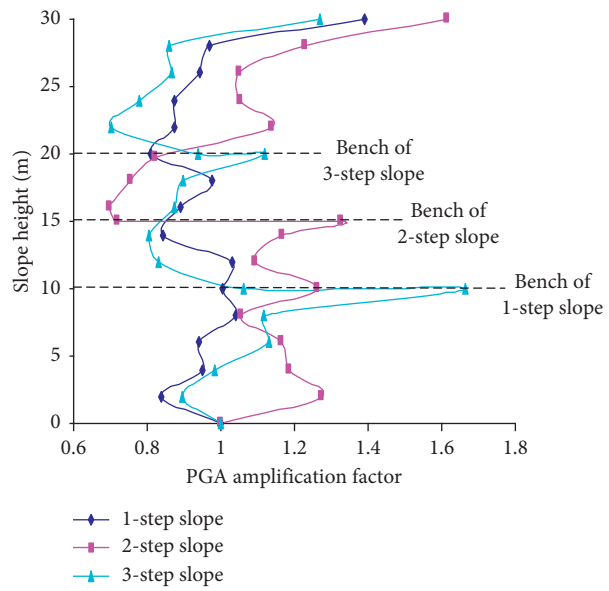

Figure 5: PGA amplification factor at monitoring points on slopes with different steps.

step presents a similar change law with that of the bench of the second step of the slope: fluctuating while increasing from slope toe to slope shoulder and reaching the peak at slope shoulder. Under Condition J-2, i.e., the condition of the 2-step slope, two rhythms occur to the PGA amplification factor. Under Condition J-3, i.e., the condition of the

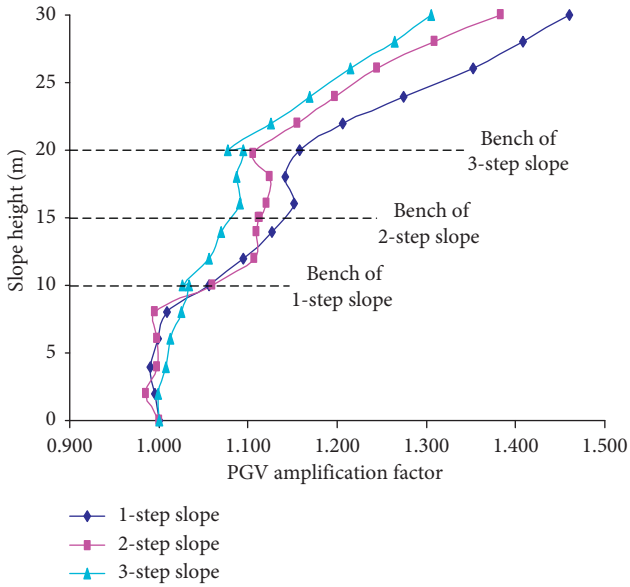

Figure 6: PGV amplification factor at monitoring points on slopes with different steps.

3-step slope, three rhythms occur to the PGA amplification factor, where the PGA amplification factors of the first and the third slope steps increase obviously, that of the second fluctuates significantly, and that at the slope shoulder of the first slope step is the maximum. According to the variation law of the PGA amplification factors of loess slopes with different steps, the PGA amplification factor of the multistep slope is rhythmic, with a rhythm corresponding to each step, which means each slope step is similar to an independent slope body. It is worth pointing out that the front-edge slope shoulder, and the rear edge, slope toe of each slope step are located at the same height, the PGA amplification factor at the monitoring point of the front edge is far larger than that of the rear edge, or rather, the PGA amplification factor at the monitoring point outside the slope is far larger than that within the slope bench; besides, a significant growth in the PGA amplification factor can be seen at the monitoring point close to slope top in spite of the step number.

Figure 6 shows that the PGV amplification factors at the monitoring points of loess slopes with different steps increase obviously with slope height in spite of the step number. From the slope toe to 1/3 slope height, the larger the step number is, the larger the PGV amplification factor will be; but from the height of the slope 1/3 to slope top, the larger the step number is, the smaller the PGV amplification factor will be. On the bench of the same slope height, the PGV amplification factor at the monitoring point of the front edge obviously differs from that of the rear edge, presenting a sharp change.

Figure 7 shows the horizontal displacements of slope monitoring points of loess slopes with different steps. It can be seen that the larger the step number is, the smaller the horizontal displacement under earthquake will be. While the maximum displacement generally occurs near 1/4 slope height, and the displacement at the slope top is also larger.

4. Dynamic Response Analysis of Loess Slopes with Different Bench Widths

To study the influence of the bench width on the dynamic response of the slope, four conditions of the bench width, i.e., 2 m, 3 m, 4 m, and 5 m, are set for a 30-meter-high three-step loess slope with two benches. That is to say, under Condition I, the two benches of the 30-meter-high three-step loess slope are both 2 m wide; under Condition II, the two benches are both 3 m wide; and so on. Through numerical simulation calculation under each condition, the distribution laws of dynamic response, including acceleration, velocity, and displacement, of loess slopes with different bench widths are obtained, as shown in Figures 8–10.

It can be seen from Figure 8 that, although the four working conditions have different bench widths, three rhythms occur to the PGA amplification factor under all four conditions and the rhythmic PGA amplification factor presents a fluctuating and increasing trend. Under different conditions of the slope with the same height, the wider the bench is, the larger the PGA amplification factor of the monitoring point will be.

It can be seen from Figure 9 that, from the toe of the first slope to the height of 1/3 slope, the PGV amplification factor increases with the slope height and the wider the bench is, the greater the increase amplitude of the PGV amplification factor will be. From the toe of the second step, i.e., 1/3 slope height, to the slope top, however, the situation gradually reverses—the narrower the bench is, the larger the PGV amplification factor will be.

It can be seen from Figure 10 that the wider the bench of a multistep loess slope is, the smaller the horizontal displacement at the monitoring points on the slope under dynamic action will be. In the case of different platform widths of the multistep loess slope, remarkable displacement occurs at the monitoring points of the front and rear edges of the first bench, and with the increase in bench width, the monitoring point where the maximum horizontal displacement occurs gets closer to the toe of the first slope step.

5. Dynamic Response Analysis of Loess Slopes with Different Slope Ratios

To study the influence of slope ratios on the dynamic response of the loess slope, the slope ratio of each grade slope is set to 1 : 0.5, 1 : 0.75, 1 : 1, and 1 : 1.25 for the third-grade slope with a height of 30 m. A slope ratio refers to the ratio of vertical height to horizontal width of a slope, i.e., the tangent value of a slope angle. The distribution laws of the dynamic response, including acceleration, velocity, and displacement, of loess slopes with different slope ratios are obtained by numerical calculation, which are shown in Figures 11–13.

It can be seen from Figure 11 that a sharp change occurs to the PGA amplification factor at the bench of each slope step under all conditions of the three-step loess slope. On the whole, the PGA amplification factor at the shoulder of the first step of slope presents an increasing trend with the decrease in the slope ratio and reaches its peak at the slope

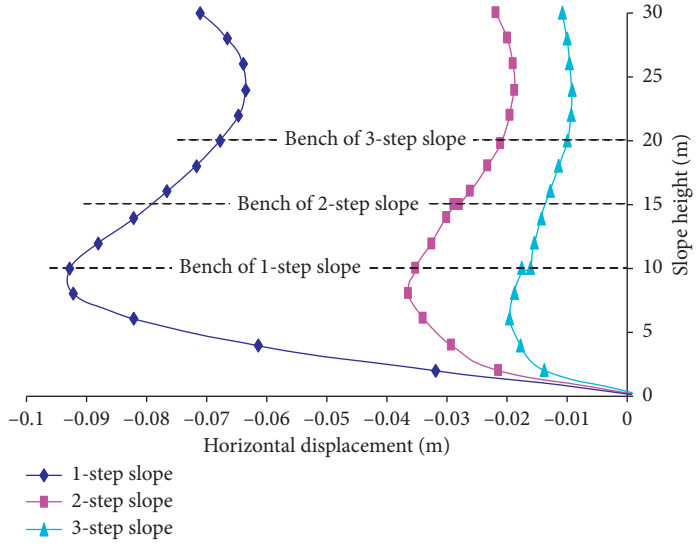

Figure 7: Horizontal displacement at monitoring points on slopes with different steps.

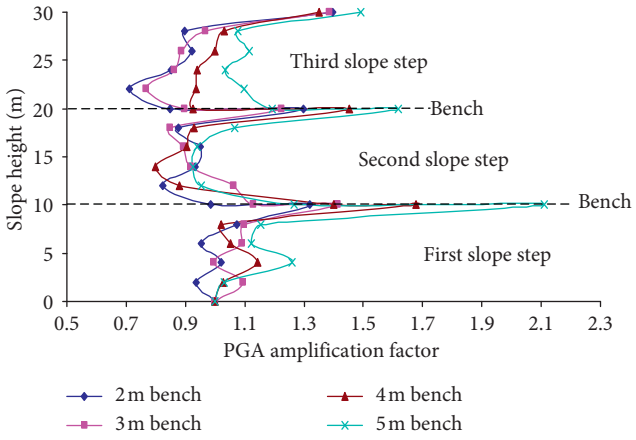

Figure 8: PGA amplification factor at monitoring points on the slopes with different bench widths.

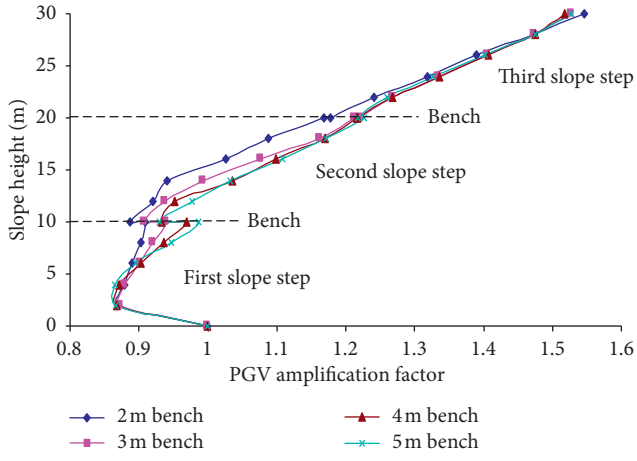

Figure 9: PGV amplification factor at monitoring points on the slopes with different bench widths.

ratio of 1 : 0.75; the PGA amplification factor at the shoulder of the second step of slope exceeds that of the first at the slope ratio of 1 : 1.25. It can be considered that the ratio 1 : 1 is a critical value—the occurrence of acceleration amplification concentrates at the first step of the slope when the slope ratio is higher than the critical value and transfers to the second and third steps of the slope when the slope ratio is lower than the critical value.

It can be seen from Figure 12 that the PGV amplification factor increases with slope height under all conditions of the slope ratio of loess slope but is relatively larger at the slope ratio 1 : 0.5. With a decrease in the slope ratio, the PGV amplification factor gets smaller and has no obvious changes at different slope ratios.

It can be seen from Figure 13 that the lower the slope ratio, the smaller the horizontal displacement of the slope. When the slope ratio decreases from 1 : 0.5 to 1 : 0.75, the slope displacement decreases significantly, but with further decrease in the slope ratio, the change in displacement gets increasingly smaller. This shows that only reducing the slope ratio plays no obvious role in improving the dynamic stability of the loess slope.

6. Conclusion

The dynamic analysis module of FLAC3D software is used to analyze the seismic dynamic response of loess slopes with different shapes, taking into account three major parameters, i.e., step number, bench width, and slope ratio, and multiple conditions are set for simulation calculation to get the following conclusion. The change in the PGA amplification factor of the multistep loess slope with slope height is rhythmic, with a rhythm occurring to each step and the distribution of the PGA amplification factor of each slope step is similar to that of an independent slope. The larger the step number is, the smaller the horizontal displacement under earthquake will be. The maximum displacement

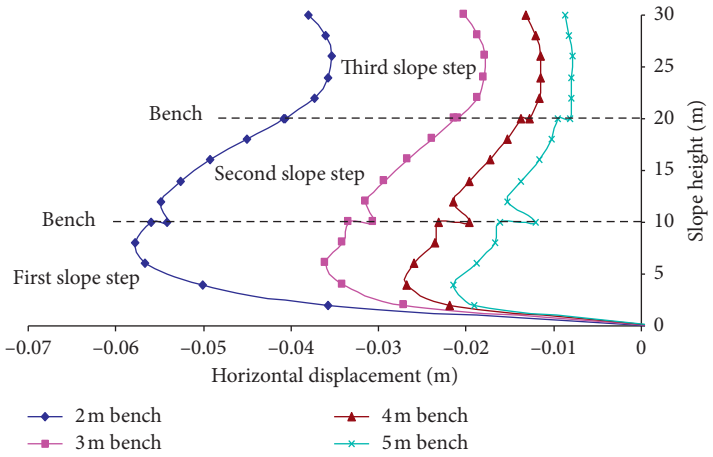

Figure 10: Horizontal displacement at monitoring points on slopes with different bench widths.

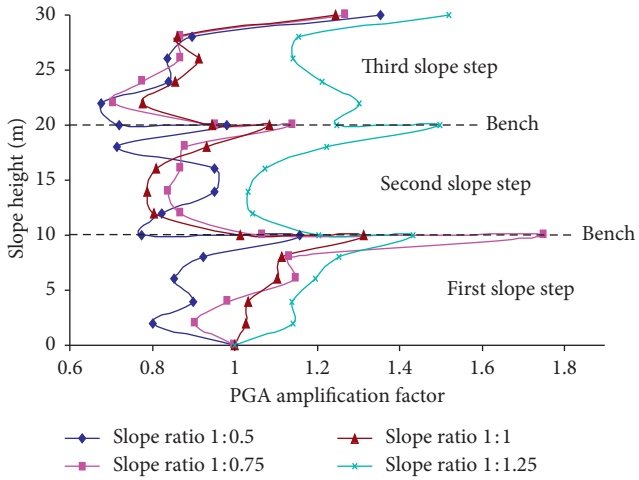

Figure 11: PGA amplification factor at monitoring points on slopes with different slope ratios.

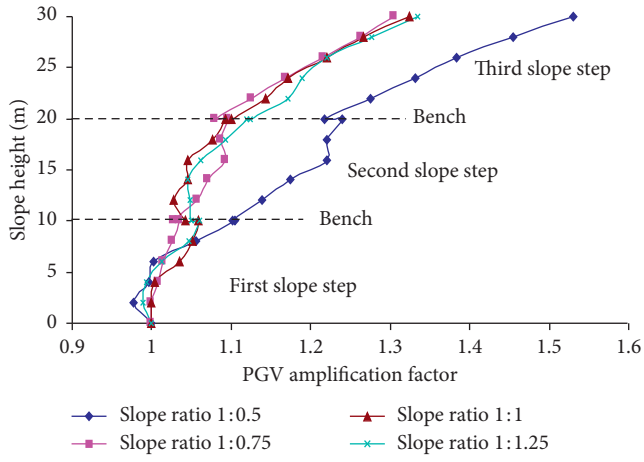

Figure 12: PGV amplification factor at monitoring points on slopes with different slope ratios.

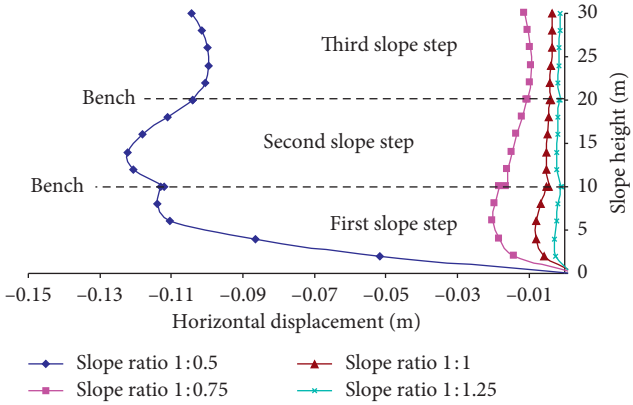

Figure 13: Horizontal displacement at monitoring points on slopes with different slope ratios.

generally occurs at around 1/4 slope height and the displacement at slope top is also large. On the bench of the same height of a multistep loess slope, the dynamic response acceleration, velocity, and displacement at the monitoring point of front edge obviously differs from those of rear edge, presenting a sharp change. For loess slopes with different bench widths, the wider the bench is, the larger the PGA amplification factor of the monitoring point will be. With the increase in bench width, the horizontal displacement of the slope decreases and the monitoring point where the maximum horizontal displacement occurs gets closer to the toe of the first slope step. The slope ratio 1 : 1 is the critical value for the change laws of the PGA amplification factors at different slope ratios, and the occurrence of acceleration amplification concentrates at the first step of slope when the slope ratio is higher than the critical value and transfers to the higher steps of slope when the slope ratio is lower than the critical value. When the slope ratio decreases from 1 : 0.5 to 1 : 0.75, an evident reduction occurs to the PGV amplification factor and displacement of slope, but with further decrease in the slope ratio, the changes in PGV amplification

factor and displacement get smaller. Therefore, the dynamic stability of the loess slope cannot be improved simply by reducing the slope ratio.

Data Availability

The data used to support the findings of this study are available from the corresponding author upon request.

Conflicts of Interest

The authors declare that there are no conflicts of interest regarding the publication of this paper.

Acknowledgments

This research was financially supported by the National Natural Science Foundation of China (Grant no. 41372307), open project of the Key Laboratory of Mechanics on Disaster and Environment in Western China, Ministry of Education (Project no. klmwde201005), Yunnan Provincial Transportation Department's Science and Technology Project (Project no.2016(A)01), and Key Science and Technology Project for Construction of Gansu Province, China (Project nos. JK2013-20 and kjxm2014-42).

References

[1] N. Wang and L. Tang, "Motion mechanism and numerical simulation of the loess collapse," *Journal of Water Resources & Architectural Engineering*, vol. 14, no. 2, pp. 152–156, 2016.

[2] C. Chen, S. Shao, and W. Zheng, "Three-dimensional dynamic stability analysis of high loess slope taking the jiulongshan slope for example," *Rock and Soil Mechanics*, vol. 31, no. 1, pp. 229–232, 2010.

[3] C. Gong, Z. Liu, and D. Yang, "Analyses of dynamic response of the loess slope under construction vibrations," *Journal of Railway Engineering Society*, no. 7, pp. 1–9, 2008.

[4] P. Sun, Y. Yin, and S. Wu, "An experimental study on the initiation mechanism of rapid and long run-out loesslandslide caused by 1920 haiyuan earthquake," *Journal of Engineering Geology*, vol. 17, no. 4, pp. 449–454, 2009.

[5] R. Sassa, "Measurement of the apparent friction angle during rapid loading by the high-speed high stress ring shear apparatus -Interpretation of the relationship between landslide volume and the apparent friction during motion," *Landslide*, vol. 1, pp. 545–552, 1991.

[6] J. Wang and Z. Zhang, "A study on the mechanism of high-speed loess landslide induced by earthquake," *Chinese Journal of Geotechnical Engineering*, vol. 21, no. 6, pp. 670–674, 1999.

[7] D. V. Keefer, "Landslides caused by earthquakes," *Geological Society of America Bulletin*, vol. 95, no. 4, p. 406, 1984.

[8] A. Prestininzi and R. Romeo, "Earthquake induced ground failures in Italy," *Engineering Geology*, vol. 58, no. 3-4, pp. 387–397, 2000.

[9] A. E. Scheidegger, "On the prediction of the reach and velocity of catastrophic landslides," *Rock Mechanics*, vol. 5, no. 4, pp. 231–236, 1973.

[10] R. W. Jibson and D. K. Keefer, "Analysis of the seismic origin of landslides: examples from the New Madrid seismic zone," *Geological Society of America Bulletin*, vol. 105, no. 4, pp. 521–536, 1993.

[11] R. Romeo, "Seismically induced landslide displacements: a predictive model," *Engineering Geology*, vol. 58, no. 3-4, pp. 337–351, 2000.

[12] L. Deng and W. Fan, "Research on dynamic response effects of loess slop," *Journal of Engineering Geology*, vol. 20, no. 4, pp. 483–490, 2012.

[13] C. Gong, Q. Cheng, and Z. Liu, "Model test study of dynamic responses of loess slope by dynamic compaction," *Rock and Soil Mechanics*, vol. 32, no. 7, pp. 2001–2006, 2011.

[14] Z. Liu and Z. Yan, "Limit equilibrium slice method for unsaturated clay slope under rainfall infiltration," *Rock and Soil Mechanics*, vol. 37, no. 2, pp. 350–3566, 2016.

[15] Z. Yan, L. Zhang, P. Jiang et al., "Dynamic response of anchoring overlying red clay rock slope under earthquake action," *Rock and Soil Mechanics*, vol. 35, no. 3, pp. 753–758, 2014.

[16] Z. Liu, Z. Yan, S. Ling et al., "Sensitivity analysis and influence of mechanical parameters on shear strength of unsaturated soil slope," *Journal of Central South University (Science and Technology)*, vol. 43, no. 11, pp. 4508–4513, 2012.

[17] Z. Yan, B. Guo, X. He et al., "Study of effect of platform width on dynamic response and failure mechanism of stepped slopes under earthquake," *Rock and Soil Mechanics*, vol. 33, no. s2, pp. 352–358, 2012.

[18] X. Zhang, *Research on Dynamic Response of Loess Slope*, Lanzhou University, Lanzhou, China, 2011.

[19] T. T. Bui, A. Mesbah, S. Maximillien et al., "Behavior of rammed earth walls under compression or shear stress," *Journal of Materials & Environmental Science*, vol. 7, no. 10, pp. 3584–3594, 2016.

[20] R. El-Nabouch, Q.-B. Bui, P. Perrotin, and O. Plé, "Shear parameters of rammed earth material: results from different approaches," *Advances in Materials Science and Engineering*, vol. 2018, Article ID 8214604, 9 pages, 2018.

[21] H. Su, Y. Hang, Y. Song, K. Mao, D. Wu, and X. Qiu, "Seismic response of anchor + hinged block ecological slope by shaking table tests," *Advances in Materials Science and Engineering*, vol. 2018, Article ID 7684831, 13 pages, 2018.

[22] C. Peng, D. Qian, L. Zhao, F. H. Ren, and Z. Y. Qian, "Stability analysis of dump slope based on FEM strength reduction method," *Applied Mechanics and Materials*, vol. 501–504, pp. 51–55, 2014.

[23] L. Zhang, Y. Zheng, S. Zhao et al., "The feasibility study of strength-reduction method with FEM for calculating safety factors of soil slope stability," *Journal of Hydraulic Engineering*, vol. 1, no. 1, pp. 21–26, 2003.